Rough-smooth-rough dynamic interface growth in supported lipid bilayers

Piyush Verma, Morgan D. Mager, and N. A. Melosh
Materials Science and Engineering, Stanford University, 476 Lomita Mall, Stanford, California 94305, USA
(Received 20 February 2013; revised manuscript received 12 September 2013; published 13 January 2014)

The role of lipid bilayer viscoelasticity and the substrate-bilayer interactions on the spreading behavior of supported phospholipid bilayer membranes is studied using fluorescence microscopy. Unlike the monotonic roughening observed on silica or in other dynamic interface growth systems, a unique rough-smooth-rough (RSR) interface transition occurred on chromium oxide with a roughness exponent of 0.45 ± 0.04. This RSR transition is attributed to the elasticity of the lipid bilayer which is initially under compression due to surface interactions, and is well approximated by adding an elastic term to the quenched noise Edwards-Wilkinson equation. A phase diagram depicting the conditions necessary to observe RSR transitions in dynamic interface systems is derived, revealing the classes of dynamically evolving systems is broader than previously thought, and the viscoelastic nature of the lipid bilayer may play a role in supported membrane behavior.

DOI: 10.1103/PhysRevE.89.012404 PACS number(s): 68.08.−p, 87.14.Cc, 81.05.Lg

I. INTRODUCTION

Two-dimensional fluid flows often exhibit rich and complex phenomena through dynamic pattern formation driven by interfacial interactions. Phospholipid bilayers are remarkable two-dimensional viscoelastic materials, which are used extensively as model cell membranes [1,2]. Lipid bilayers are often prepared on solid surfaces for convenient handling and imaging; however, the inherent elasticity of the bilayer is generally disregarded. Much of the understanding of dynamic lipid behavior comes from lipid spreading experiments, which measure the displacement, velocity, and roughness of the bilayer edge or the dynamic wetting line as it expands from a large source of lipid. Experiments on silica, MgF_2, and mica found the bilayer edge expansion behaves according to the well-known class of dynamic interface growth models [2,3]. Dynamic evolution of interfaces with quenched disorder are common in nature [4], including fluid flow in porous media [5,6], granular particle flow [7], bacterial colony growth [8], and motion of domain walls in magnetically ordered systems [9,10]. These interfaces, which are either modeled using the quenched noise-Kardar-Parisi-Zhang (KPZ) equation or the quenched noise-Edwards-Wilkinson (QEW) equation [11], expand due to a driving force while the edge profile roughens monotonically over time due to a distribution of disordered, trapping defects. These systems do not have elastic expansion or restoring forces, which may yield new phenomena in interface growth. For lipid bilayers, elasticity may play a role during expansion as observed in static lipid bilayers [12], yet no evidence for this has been found in previous dynamic expansion experiments. However, these experiments have used large lipid droplets as the material source, creating an infinite source that can mask the effects of elasticity [2,3,13].

Here we demonstrate that bilayer elasticity plays an important role in dynamic lipid behavior on solid surfaces, and suggests significant compression may be present in the most common vesicle-rupture bilayer preparation technique. Moreover, under certain ranges of bilayer interaction energy and compressibility the edge roughness of the expanding bilayer undergoes a rough to smooth to rough (RSR) transition. This unique transition can be quantitatively modeled by adding an elastic term into the QEW equation, supporting elasticity as the determining factor. The monotonic roughening of canonical dynamic evolution models is thus seen as a limiting case for physical systems where restoring forces are not present. A phase diagram of the lipid interface roughness behavior was constructed from numerical simulations, revealing that the relative magnitudes of surface interaction energy, elastic modulus, and trap depth control the edge roughening characteristics for this class of systems.

II. EXPERIMENT

Lipid expansion experiments were performed on two different surfaces, silica and chromium oxide, which are expected to have different interaction energies with the lipid bilayer. Chromium oxide surfaces were prepared by *e*-beam evaporation of 50 nm of chromium deposited at 1 Å/s onto a freshly cleaned glass slide and oxidized with UV ozone treatment for 15 min. For silica surfaces, either a glass microscope slide or thermally oxidized silicon wafer were piranha cleaned, rinsed, and blown dry immediately prior to use. Vesicle rupture bilayers were deposited with standard protocols [12,14]. In this method, first a 10 mg/ml organic solution of phospholipid (POPC) (Avanti Polar Lipids, Alabaster, AL) with 1% mole fraction of fluorescent Texas-Red lipids in chloroform was prepared. Once the lipids were thoroughly mixed in the organic solvent, the solvent was removed to yield a lipid film by using a dry nitrogen stream in a fume hood. To remove any residual organic solvent, the lipid film was dried completely by placing the vial in a desiccator under vacuum overnight. The lipid film was then hydrated by adding phosphate buffered saline solution followed by vigorous mixing on a minivortexer for 1 h. The lipid vesicles were produced by the extrusion of multilamellar POPC vesicles through a 100-nm polycarbonate membrane and were used at a concentration of 5 mg/ml. Bilayers were deposited on both surfaces by vesicle rupture of these phospholipid (POPC) vesicles. About 100 μl of the lipid vesicle solution was dropped on the clean surface of the substrate and a glass cover slip was placed on top. The substrate was then immersed under de-ionized water and allowed to stand for 10 min. The osmotic pressure difference between the inside and outside media of the vesicles and the interaction with the substrate surface caused the vesicles to

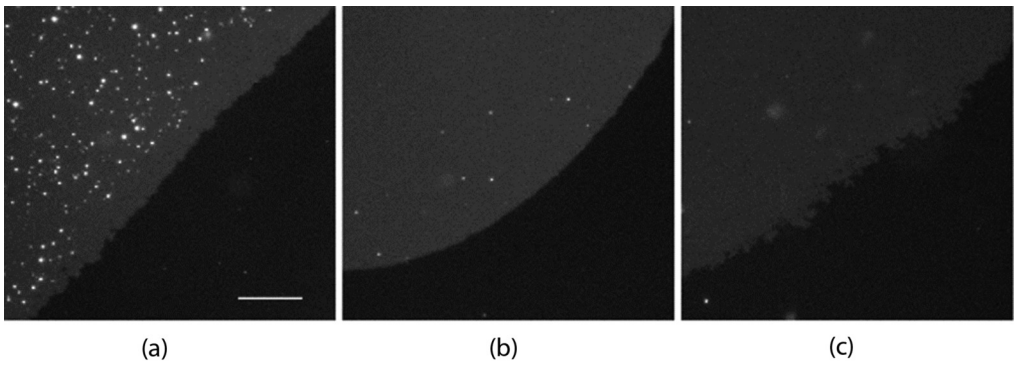

FIG. 1. Snapshots of the advancing bilayer interface as it expands on chromium oxide at (a) $t = 30$ min, (b) $t = 190$ min, (c) $t = 48$ h. The roughness at the scale of a few μm reduces in the beginning (smoothing) and then increases towards the end (roughening). Scale bar in (a) is 10 μm. Bright spots in the images are unruptured lipid vesicles.

rupture and form a supported bilayer. To dislodge most of the excess unruptured vesicles adhered to the substrate, the surface was subjected to a stream of de-ionized water created using a pipette nozzle while submerged in solution.

A part of the bilayer was then removed cleanly by blowing a localized high speed stream of air bubbles from a pipette onto the preformed bilayer. The high surface energy of the air-water interface drives the lipids to rapidly adsorb onto the bubble surface and dislodge from the substrate [15]. This process avoids scratching or deposition of foreign material that may alter the lipid behavior. The expansion of the lipid bilayer into the now clean region was recorded with time lapse fluorescent microscopy (Fig. 1). We used a Zeiss (Oberkochen, Germany) axioimager upright fluorescence microscope with a 63 × /0.75NA water immersion objective lens and pictures were captured using the AxioCam MRm (Zeiss Oberkochen, Germany). After acquisition, the coordinates of the interface were extracted with ImageJ software (NIH, Bethesda, MD) and large-scale features removed by subtracting a smooth spline fit of the digitized interface, similar to previous work [2]. Figure 2(a) shows a series of the lipid interface position as a function of expansion time. Average displacements were calculated from the interface position relative to the starting location, and the interface velocity computed as a forward difference from the displacement data.

III. OBSERVATIONS

We observed that as the bilayer expanded spontaneously on chromium oxide, the interface edge rapidly smoothened, reached a transition point, then roughened at a slower rate. The edge roughness was quantified by the interfacial width or RMS roughness with time [7]:

$$w(L,t) = \sqrt{1/L \sum_{i=1}^{L} [h(i,t) - \bar{h}(t)]^2},$$

where h is the digitized column height of the interface from its initial position, i the column number, and L the total number of columns (pixels). As shown in Fig. 2(b), the initially rough interface reached a minimum roughness near 200 min, then almost completely recovered after 3000 min at an average rate more than ten times slower than the smoothening process. The RSR transition can also be clearly seen in the fluorescence microscope images in Fig. 1. This behavior is quite distinct from lipid expansion on either silica surface, where only monotonic roughening is observed.

Another significant difference is the shape of the velocity profile of the advancing bilayer which transitions from $t^{-1/2}$, as expected for a uniform driving force [2], to a $t^{-7.75}$ regime as shown in Fig. 3(b). Some indication of this transition also appears to be present in the long time limit of the velocity data reported by Radler and co-workers for a bilayer spreading on mica [2].

To compare to other dynamic growth phenomena, the roughness exponent was extracted from the interface coordinates. The height-height correlation function is given by

$$C(l) = \sqrt{\langle [h(x) - h(x')]^2 \rangle}, \quad |x - x'| = l,$$

where l is the system size, and x is the transverse direction. This is plotted for different surfaces in Fig. 2(c). For self-affine interfaces, $C(l) \propto l^{2\alpha}$ for $l \ll \xi^{\|}$ where α is the roughness exponent and $\xi^{\|}$ is the horizontal correlation length [4]. The universality constant α is typically 0.6–0.9 in quenched disorder systems, with $\alpha = 0.81 \pm 0.04$ on silica with an infinite lipid source [3,16]. This value largely depends upon the value of the driving force relative to the other forces in the system [17]; for example, it is predicted to vary with pressure in Hele-Shaw cells [18,19]. The bilayer edge advancing on chromium oxide had $\alpha = 0.45 \pm 0.04$, and was constant over the course of the experiment, even though the edge roughness was changing dramatically as shown in Fig. 2(c). On glass the interface monotonically roughened with $\alpha = 0.87 \pm 0.05$, while on thermally oxidized silicon it was slightly lower, $\alpha = 0.73 \pm 0.08$. This is a large change in universality constant between chromium oxide and glass, indicating that the relative driving forces may be quite different.

IV. MODELING AND RESULTS

To estimate these forces, a modified version of the QEW equation, including an elastic spring term for the bilayer elasticity, was constructed. The modified equation balances the viscous drag, elasticity, interfacial energy, and line tension

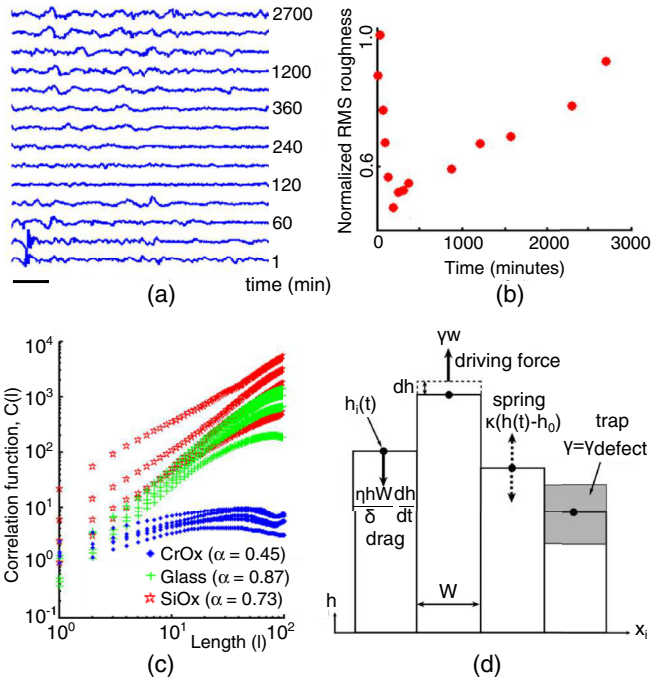

FIG. 2. (Color online) (a) The position of the bilayer edge on chromium oxide surface at proceeding time. The edge has been straightened out by subtracting a spline fit. Note rough to smooth to rough transition. Data arbitrarily offset for clarity. Scale bar below the trace marked "1 min" is 10 μm. (b) The normalized interface width (RMS roughness) normalized to the initial roughness as a function of time shows a distinct dip confirming the rough-smooth-rough transition. (c) Log-log plot of the height-height correlation function $C(l)$ as a function of distance between points at which height is measured (l). The initial slope gives the roughness exponent of the interface. Different colors correspond to different bilayer-substrate systems: red (top traces) for silicon oxide surface, green (middle traces) for glass surface, and blue (bottom traces) for chromium oxide surface. Different traces of the same color are for the interface at different time points. Bilayer edge on chromium oxide shows an anomalously low α of 0.45 $\pm$ 0.04. On silicon oxide and glass, the roughness exponent lies in range observed for other systems with quenched disorder, 0.73 $\pm$ 0.08 and 0.87 $\pm$ 0.05, respectively. (d) Schematic showing the spring force, the viscous drag, and the substrate-bilayer interaction force acting on the expanding bilayer, depicted here as growing columns. The force due to bilayer line tension has been omitted for clarity.

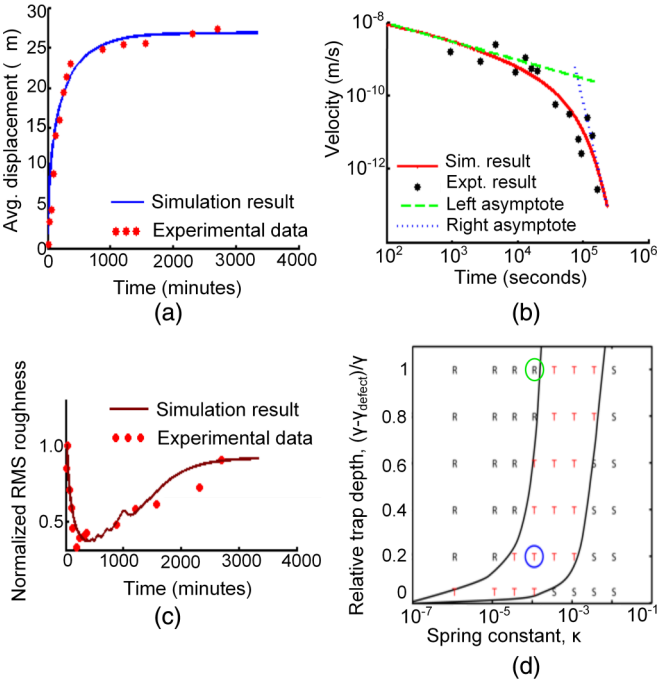

FIG. 3. (Color online) (a) Average displacement of the advancing bilayer edge on chromium oxide surface plotted against time. Simulation results overlaid on experimental data. (b) Log-log plot of the average velocity of the advancing bilayer edge on chromium oxide overlaid on the simulation results. The left asymptote corresponds to the case without the spring term. (c) Time evolution of the interface width or RMS roughness shown for experiment and simulation. Simulation clearly captures the rough-smooth-rough transition on chromium oxide surface. (d) Phase diagram depicting the narrow parameter space necessary for RSR transition. R, T, and S denote roughening, transition, and smoothening, respectively. The x axis is the spring constant of the bilayer in logarithmic scale and the y axis is the pinning strength of the defects. The blue circle (bottom) denotes bilayer–chromium oxide system and green (top) denotes the bilayer-glass system.

with quenched noise:

$$\frac{\eta A}{\delta}\frac{\partial h}{\partial t} = \gamma w - \lambda\frac{dl}{dh} + \eta(x,h) - \kappa\,(h - h_0)\ldots, \qquad (1)$$

where the interface is characterized by a height $h(x,t)$ moving in a two-dimensional disordered medium with quenched noise $\eta(x,h)$. The substrate-bilayer interaction force is the product of the interaction energy, γ, and the width of the bilayer normal to the growth direction, w. The drag force is assumed to arise due to the velocity gradient in the fluid cushion under the bilayer. Assuming Newtonian behavior, this can be calculated using the fluid viscosity η, cushion thickness δ, and area of contact A. The line tension force is modeled as the derivative of the change in edge energy, λdl with respect to the displacement of the edge, h. Here, l is the length of the bilayer interface and λ is the bilayer line tension. This model is shown schematically in Fig. 2(d).

For quenched noise Edwards-Wilkinson (EW) systems without an elastic force and a negligible line tension term, the differential equation (1) can be solved to show that edge velocity $v(t)$ is proportional to $t^{-1/2}$ [2]. In this case, the drag force which is proportional to the product of the displacement and velocity is invariant over the course of expansion. If the driving force is smaller than the viscous drag and trap depth put together, the defects will pin a part of the interface and roughening occurs. Since the competition between the driving force and the retarding forces is not dynamic in nature, the interesting RSR transition is not observed.

In our model, the dependence of elastic force on the displacement of the bilayer edge dynamically changes the driving force through the course of expansion. When the initial state is under compression, the elastic force provides additional driving force so that the interface is able to either overcome or rapidly fill in behind any defect sites on the surface. If the

interface is rough to begin with, it smoothens in this expansion regime. As the interface continues to expand further, the elastic force goes on reducing until it becomes comparable to the substrate-bilayer interaction force. Any defect sites on the substrate are now able to reduce the interface velocity locally. This marks the onset of roughening and is the transition point at which the roughness trend reverses. If the transition occurs at an interface displacement of h_{trans}, then

$$\kappa(h_0 - h_{\text{trans}}) = \gamma w - \lambda \frac{dl}{dh},$$

where γ_{def} is the substrate-bilayer interaction energy at a defect site. For a model with discrete columns of lipid that grow over time [Fig. 2(d)], the maximum value of $\lambda dl/dh$ for unequal columns is 2λ, thus

$$h_0 - h_{\text{trans}} = \frac{\gamma w - 2\lambda}{k} \ldots . \tag{2}$$

A compressed initial state of the bilayer can be seen as a direct result of the favorable substrate-bilayer interaction. Due to this favorable interaction, the overall energy of a bilayer is reduced by packing a higher number of lipid molecules per unit area of the substrate. This compression is estimated to be about 6% from experiments carried out by Cremer *et al.* [12].

The modified QEW equation was numerically integrated on a rectangular grid following Kessler *et al.* [18]. The interface was initialized by a random deposition process and the defects were modeled by a constant pinning force rather than a Gaussian distribution. The bilayer edge tension λ was assumed to be 1×10^{-11} J/m, which has been reported from experiments involving pore formation of vesicles [20]. The water cushion thickness δ, determined by experiments involving neutron reflectivity, was assumed to be 1 nm [21]. The viscosity of the water cushion was scaled up by a factor of 10^5 with respect to the bulk value at room temperature (0.1 cP). This viscosity enhancement factor is in agreement with the results reported for flows confined to very small volumes. Atomic force microscopy on thin water layers further corroborates an enhancement factor in the range of 10^3–10^5 [22,23].

Results from the model were fit to the experimental roughness data and displacement profile of the advancing interface [Figs. 3(a) and 3(c)] to estimate the spring constant κ, the free length of the spring h_0, the specific interaction energy between the bilayer and the substrate, γ, and the interaction energy at defect sites, γ_{defect}. These are reported in Table I. The fraction of defect sites was arbitrarily set at 10% since the results were found to be relatively insensitive to this parameter. The bilayer-substrate interaction energy γ for POPC on chromium oxide was found to be around ten times lower than that on glass. The value of γ on glass was found to within an order of magnitude of the other reported estimates [24]. For the same defect fraction, the trap depth on glass was found to be much higher than that on chromium oxide. The spring constant for the bilayer, κ was found to be 10^{-4} N/m for both surfaces. Assuming an isotropic area expansion, the area expansion modulus of the bilayer, K_A, can be estimated as 0.02 N/m. Compared to giant vesicle micropipette experiments and molecular dynamics simulations, this value is about an order of magnitude smaller [25,26]. The neutral length of the spring, h_0, was found to be about two orders of magnitude higher on glass than on chromium oxide. This is believed to be due to the much higher total bilayer area on glass as compared to that on chromium oxide. Plugging these values into Eq. (2) for the chromium oxide case, h_0–$h_{\text{trans}} \sim 1$ μm. Thus, at the transition, the interface displacement, h_{trans}, should be about 25 μm for $h_0 = 26$ μm. This is very close to an edge displacement of 23 μm measured from experiment [Fig. 3(a)].

TABLE I. Experimental parameters for the silica-bilayer and chromium oxide–bilayer systems obtained using numerical simulations.

	Glass	Chromium oxide
γ (mJ/m^2)	$\sim$1	$\sim$0.4
κ (N/m)	10^{-4}	10^{-4}
$(\gamma - \gamma_{\text{defect}})/\gamma$	$\sim 10^2$	10^{-1}
h_0 (μm)	4500	26

The competition between the smoothening action of the spring force and the roughening due to pinning sites is illustrated by the phase diagram in Fig. 3(d). This was prepared by simulating bilayer spreading on surfaces with varying relative trap depth, $(\gamma - \gamma_{\text{defect}})/\gamma$, for a range of spring constant values, keeping the defect fraction constant. The diagram shows that large lipid elastic moduli with weak defect pinning on the substrate result in monotonic smoothening of the interface, as is depicted by the regions marked "S" in the phase diagram. In this region, the driving force is high enough to overcome the trap sites. However, due to a high spring constant, the driving force falls sharply with displacement and the expansion comes to a halt before the interface shows any measurable roughening. This region suggests that there could be a system that may have such a smoothening regime, which has not yet been observed experimentally. For strong pinning sites and weak springs, monotonic roughening of the interface is seen (marked by "R"). The driving force in this region is always lower than the trap energy. The corresponding region for the phase diagram on glass is the region that has been explored in previous studies of bilayer spreading [2,3,13]. Within a narrow regime sandwiched between the S and R regions, marked by "T" for transition, is where the RSR transition occurs. It is only in this parameter space that the roughening and smoothening forces are identical in magnitude and the effect of each is seen clearly. The chromium oxide–bilayer system is found to lie in this transition region.

V. CONCLUSIONS

The role of lipid bilayer viscoelasticity in the spreading behavior of supported phospholipid bilayer membranes is clearly important. Since vesicle rupture bilayers are routinely used as physiological mimics of the cell membrane, a more complete understanding of the influence of the roughly $\sim$4% compression should be undertaken. This compressive strain could have an effect on the activity of proteins incorporated in the bilayer, thus influencing the quality of biosensors based on this platform. In-plane diffusivity measurements

of the lipid bilayer are also likely to be affected by this compression.

The lipid–chromium oxide system with $\alpha \sim 0.45$ suggests an addition to the family of universality classes already known. The occurrence of the RSR transition reveals how unique phenomena can emerge due to the addition of external modulating forces, such as the restoring force in this case. Furthermore, the EW equation which is considered standard for the description of linear systems was found to be inadequate to capture the dynamics of lipids on chromium oxide. The modified EW equation proposed in this work includes the effect of restoring forces and makes the EW equation more generally applicable.

[1] E. Sackmann, Science **271**, 43 (1996).
[2] J. Radler, H. Strey, and E. Sackmann, Langmuir **11**, 4539 (1995).
[3] J. Nissen, K. Jacobs, and J. O. Radler, Phys. Rev. Lett. **86**, 1904 (2001).
[4] A.-L. Barabási and H. E. Stanley, *Fractal Concepts in Surface Growth* (Cambridge University Press, Cambridge, 1995).
[5] M. A. Rubio, C. A. Edwards, A. Dougherty, and J. P. Gollub, Phys. Rev. Lett. **63**, 1685 (1989).
[6] P. de Gennes, Rev. Mod. Phys. **57**, 827 (1985).
[7] Z. Csahók and T. Vicsek, Phys. Rev. A **46**, 4577 (1992).
[8] T. Vicsek, M. Cserzo, and V. K. Horvath, Physica A **167**, 315 (1990).
[9] R. Bruinsma and G. Aeppli, Phys. Rev. Lett. **52**, 1547 (1984).
[10] M. Jost and K. D. Usadel, Phys. Rev. B **54**, 9314 (1996).
[11] D. R. Wilkinson and S. F. Edwards, Proc. R. Soc. London, Ser. A **381**, 33 (1982).
[12] P. S. Cremer and S. G. Boxer, J. Phys. Chem. B **103**, 2554 (1999).
[13] B. Sanii and A. N. Parikh, Soft Matter **3**, 974 (2007).
[14] A. A. Brian and H. M. McConnell, Proc. Natl. Acad. Sci. USA **81**, 6159 (1984).
[15] M. D. Mager and N. A. Melosh, Langmuir **23**, 9369 (2007).
[16] L. A. Nunes Amaral, A.-L. Barabási, H. A. Makse, and H. E. Stanley, Phys. Rev. E **52**, 4087 (1995).
[17] V. K. Horváth and H. E. Stanley, Phys. Rev. E **52**, 5166 (1995).
[18] D. A. Kessler, H. Levine, and Y. Tu, Phys. Rev. A **43**, 4551 (1991).
[19] S. He, G. L. M. K. S. Kahanda, and P.-z. Wong, Phys. Rev. Lett. **69**, 3731 (1992).
[20] D. V. Zhelev and D. Needham, Biochim. Biophys. Acta **1147**, 89 (1993).
[21] B. W. Koenig, S. Krueger, W. J. Orts, C. F. Majkrzak, N. F. Berk, J. V. Silverton, and K. Gawrisch, Langmuir **12**, 1343 (1996).
[22] R. C. Major, J. E. Houston, M. J. McGrath, J. I. Siepmann, and X.-Y. Zhu, Phys. Rev. Lett. **96**, 177803 (2006).
[23] T.-D. Li, J. Gao, R. Szoszkiewicz, U. Landman, and E. Riedo, Phys. Rev. B **75**, 115415 (2007).
[24] J. Marra and J. Israelachvili, Biochemistry **24**, 4608 (1985).
[25] W. Rawicz, K. C. Olbrich, T. McIntosh, D. Needham, and E. Evans, Biophys. J. **79**, 328 (2000).
[26] J. Jeon and G. A. Voth, Biophys. J. **88**, 1104 (2005).